J. Chem. Sci., Vol. 123, No. 1, January 2011, pp. 21–27. © Indian Academy of Sciences.

A quasiclassical trajectory analysis of stereodynamics of the H + FCl ($v = 0-3$, $j = 0-3$) → HCl + F reaction

XIAN-FANG YUE[a]* and XIANGYANG MIAO[b]

[a]Department of Physics and Information Engineering, Jining University, Qufu 273155, China

[b]College of Physics and Information Engineering, Shanxi Normal University, Linfen 041004, China

e-mail: xfyuejnu@gmail.com

MS received 5 March 2010; revised 21 October 2010; accepted 4 November 2010

Abstract. The chemical stereodynamics for the title reaction are studied by the quasiclassical trajectory method. Employing the recent works of Deskevich, Hayes, Takahashi, Skodje, and Nesbitt (DHTSN) potential energy surface of the ground $1^2A'$ electronic state, the present work calculates the polarization-dependent differential cross sections and the three angular distributions which describe the vector correlations among the product angular momentum **j′** and the reagent and the product initial relative velocities **k** and **k′**. The effect of vibrational and rotational excitations for the reagent FCl and the influence of collision energies on the stereodynamical quantities are also investigated and discussed.

Keywords. Quasiclassical trajectory method; chemical stereodynamics; polarization-dependent differential cross sections.

1. Introduction

In recent years, the FHCl reactive system has attracted a number of experimental and theoretical studies to explore its reaction dynamics for several reasons.[1–13] Firstly, it can serve as a prototype for the heavy–light–heavy mass combination reactions with two heavy halogen atoms involved. Secondly, it can be chosen as a model system to unravel reaction mechanism associated with reactive resonances.[14,15] Thirdly, it can provide excellent opportunities, just like the thoroughly studied hydrogen abstraction reactions such as F(^{2}P) + H_2 and Cl(^{2}P) + H_2,[16–28] to perform non-adiabatic dynamics studies by considering the three electronic states of $1^2A'$, $1^2A''$ and $2^2A'$ for the FHCl system. Lastly, it can provide opportunities to make detailed comparison between the previously studied reactions of halogen atoms with hydrogen molecule for deeper understanding the chemical reaction dynamics.

In 1999, Sayós *et al*. reported their analytical potential energy surface (PES) of the ground $1^2A'$ state.[1] The PES was derived from a grid of approximately 3400 *ab initial* [PUMP2/6-311G(3d2f, 3p2d)] points. Based on this PES, they calculated thermal rate constants for the H + ClF → F + HCl, Cl + HF and F + HCl → Cl + HF reactions and their deuterium isotope variants by means of the variational transition state theory with the inclusion of a microcanonical optimized multidimensional tunnelling correction. Kornweitz and Persky constructed the semiempirical LEPS PES for the reactions F + HCl, F + HBr, and F + HI.[2] Employing this LEPS PES, they carried out quasiclassical trajectory (QCT) calculations to reproduce the experimental kinetic data such as rate constants, product vibrational state distributions and energy distributions among reaction products. The full 3×3 matrix of diabatic potentials for the lowest three states for the Cl(^{2}P)-HF complex was developed by Fishchuk *et al*.[3] who carried out the three-dimensional computations of the bound states of that complex. In a recent work, Deskevich, Hayes, Takahashi, Skodje, and Nesbitt developed a new ground $1^2A'$ state PES for the FHCl reactive system (denoted as DHTSN PES) from the *ab initio* calculations at the multireference configuration interaction+Davidson correction level of theory.[4] Up to now, the DHTSN PES is the most accurate ground PES, and is available to perform the dynamics calculations.

*For correspondence

On the PESs mentioned above, a lot of quantum wave packet and QCT calculations have been carried out for the FHCl system. Tang *et al*. carried out the time-dependent wave packet calculations for the F + HCl and F + DCl reactions on the PES of Sayós *et al*.[1,5] Employing the DHTSN PES, Hayes *et al*. performed the time-independent quantum and QCT calculations for the F + HCl reaction,[6] and Sun *et al*. also performed the time-dependent quantum calculations for the same reaction.[7] These calculations reveal a reactivity enhancement by vibrational and rotational excitations of the HCl molecule. Quéméner and Balakrishnan reported the time-independent quantum dynamics calculations for the F + HCl and F + DCl reactions at cold and ultracold temperatures on the DHTSN PES.[8] In their study, the effect of rotational and vibrational excitations of the reagent molecule on the reactivity, the effect of tunnelling and Coriolis coupling, and Feshbach resonances were investigated in detail at low energies. Experimentally, previous studies show measured temperature-dependent rate constants and product rotational and vibrational distributions for the F + HCl reaction.[9–13]

Most of the previous dynamics studies for the F(^{2}P) + HCl reaction and its isotope variants mainly focused on the scalar properties such as the temperature-dependent rate constant, the product vibrational and rotational distributions, the integral cross sections and so on. However, very few theoretical studies concerned the H + FCl reaction, especially for the dynamics (particularly stereodynamics), almost no investigations on this reaction has been reported so far. In the present work, we carried out the first QCT calculations for the H + FCl (v = 0–3, j = 0–3) → F + HCl reaction at three collision energies of 20, 30 and 40 kcal/mol. The state-to-state reaction dynamics and chemical stereodynamics are revealed in this paper. The present QCT calculations are performed on a benchmark QCT procedure, which is developed by Han's group and available to study both the vector and scalar properties for triatomic chemical reactions.[29–34] In 1993, Han *et al*. carried out the first QCT calculations on the product alignment with this procedure, which made it possible to compare theoretical rotational polarization and experimental one directly.[34] Subsequently, the QCT procedure was gradually developed and optimized to study the chemical stereodynamics to other reaction system.[29–33] Many other theoretical methods were also developed to study the chemical stereodynamics, and the excellent work has been done by Aquilanti and co-workers,[35,36] Aoiz and co-workers,[37,38] Roncero and co-workers and Balint–Kurti and co-workers.[39–43]

2. Computational aspects

In our calculations, the Hamilton's equations are solved by using a six-order symplectic integrator method. The integration step is set to 0·1 fs for the converged calculated results. The initial distance between the attacking atom H and the center of mass of the diatomic molecule FCl is set to 10 Å. For each of the collision energy, 50000 trajectories are running on the ground PES of the FHCl system. With initial vibrational number v = 0 and initial rotational number j = 0, the optimized maximum impact parameters are 2·25, 2·25 and 2·32 Å corresponding to the three collision energies of 20, 30 and 40 kcal/mol, respectively. For the initial rotational number j = 0 and collision energy of 20 kcal/mol, the optimized maximum impact parameters are 2·46, 2·63 and 2·66 Å corresponding to the initial vibration number v = 1, 2, and 3, respectively. While for the initial v = 0, the optimized maximum impact parameters are changed to be 2·28, 2·3 and 2·28 Å corresponding to the initial j = 1, 2, and 3, respectively. The initial orientation of the reagent angular momentum $\boldsymbol{j}$ is randomly sampled in the QCT procedure, while correlations between the product angular momentum vector $\boldsymbol{j'}$ with the reagent and the product relative velocities $\boldsymbol{k}$ and $\boldsymbol{k'}$ can be depicted by the following calculated stereodynamical quantities:

$$P(\theta_r) = \frac{1}{2}\sum_k [k] a_0^k P_k(\cos\theta_r), \tag{2.1}$$

with $[k] = 2k+1$, $a_0^k = \langle P_k(\cos\theta_r)\rangle_{reactive-trajectories}$.

$$P(\phi_r) = \frac{1}{2\pi}\left(1 + \sum_{n(even\geq 2)} a_n \cos n\phi_r + \sum_{n(odd\geq 1)} b_n \sin n\phi_r\right), \tag{2.2}$$

with $a_n = 2\langle \cos n\phi_r\rangle_{reactive-trajectories}$ and $b_n = 2\langle \sin n\phi_r\rangle_{reactive-trajectories}$.

$$P(\theta_r,\phi_r) = \frac{1}{4\pi}\sum_k \sum_{q\geq 0}\left(a_{q\pm}^k \cos q\phi_r - a_{q\mp}^k i \sin q\phi_r\right) C_{kq}(\theta_r, 0), \tag{2.3}$$

where $a_{q\pm}^k = 2\langle C_{kq}(\theta_r,0)\cos q\phi_r\rangle_{angles}(k = even)$ and $a_{q\pm}^k = 2i\langle C_{kq}(\theta_r,0)\sin q\phi_r\rangle_{angles}(k = odd)$.

$$\frac{1}{\sigma}\frac{d\sigma_{kq\pm}}{d\omega_t} = \frac{1}{4\pi}\sum_{k_1}\frac{[k_1]}{4\pi} S_{kq\pm}^{k_1} C_{k_1 q}(\theta_t, 0), \tag{2.4}$$

with $S_{kq\pm}^{k_1} = \langle C_{k_1 q}(\theta_t,0) C_{kq}(\theta_r,0)[(-1)^q e^{iq\phi_r} \pm e^{-iq\phi_r}]\rangle_{angles}$. C_{kq} represents the modified spherical harmonics in these equations.

The center-of-mass (CM) frame is used as the reference frame in the present work, which is shown in figure 1. The meanings of the stereodynamical quantities calculated with the above equations are depicted in figure 1. $P(\theta_r)$ describes the ***j′-k*** correlation with θ_r being the angle between ***j′*** and ***k*** vectors. $P(\phi_r)$ describes the ***k′-k-j′*** correlation with ϕ_r being the dihedral angle between the plane formed by vectors ***k′*** and ***k*** and the plane formed by vectors ***k*** and ***j′***. Hence, θ_r and ϕ_r are the polar angles defining the direction of ***j′***, and the polar plot $P(\theta_r,\phi_r)$ provides distribution information correlating with the polar angles. θ_t is the scattering angle between ***k*** and ***k′*** in the scattering plane (containing ***k′*** and ***k***). $\frac{1}{\sigma}\frac{d\sigma_{kq\pm}}{d\omega_t}$ are the polarization-dependent differential cross sections (PDDCSs). In this paper, two PDDCSs with kq = (0, 0) and (2, 0) are only calculated. As shown in figure 1, the z-axis is parallel to ***k*** in the CM frame, and the y-axis is perpendicular to the scattering plane (z–x plane). The truncated number used in the above expansions (Eqs. 2.1–2.4) of $P(\theta_r)$, $P(\phi_r)$, $P(\theta_r,\phi_r)$ and PDDCSs are k=18, n=24, k=7 and k_1=7, respectively. More details of the QCT procedure can be found in Refs. 29–33.

3. Results and discussion

Figure 2 illustrates the $P(\theta_r)$ distributions of HCl from the H + FCl (v=0, j=0) → HCl + F reaction at three collision energies of 20, 30 and 40 kcal/mol. Obviously, the calculated $P(\theta_r)$ distributions peak at θ_r= 90° for all of the three collision energies, which indicates that the product HCl molecule has a rather strong polarization behaviour with product alignment perpendicular to the initial relative velocity vector ***k***. However, such product alignment becomes weaker with the increasing collision energy. The $P(\theta_r)$ distributions of the HCl can be seen in figure 3a for the H + FCl (v = 0, 1, 2, 3, j = 0) → HCl + F reaction at the collision energy of 20 kcal/mol, and they are presented in figure 3b for the H + FCl (v = 0, j = 0, 1, 2, 3) → HCl + F reaction. As can be seen from figure 3a, the $P(\theta_r)$ distribution has only a slight overall increase when the reagent FCl molecule is excited to its vibrational levels of v = 1–3. This indicates a very slight enhancement in product alignment perpendicular to ***k*** at high initial vibrational level. Nevertheless, the calculated $P(\theta_r)$ distributions are nearly identical for the case of j = 0–3 and v = 0 (depicted in figure 3b), which means that the initial rotational excitation has no effect on the product alignment perpendicular to ***k*** at this collision energy.

The $P(\phi_r)$ distributions provide the product orientation and alignment information. They are shown in figure 4 for the HCl product from the H + FCl (v = 0, j = 0) → HCl + F reaction at three collision energies of 20, 30 and 40 kcal/mol. Figure 5a illustrates the $P(\phi_r)$ distributions for the case of initial rotational and vibrational state of v = 0–3, j = 0 at the collision energy of 20 kcal/mol, and figure 5b for the case of v = 0, j = 0–3. As shown in figure 4, a large and conspicuous peak appears at (or around) ϕ_r=270° for all the three collision energies, which indicates a marked

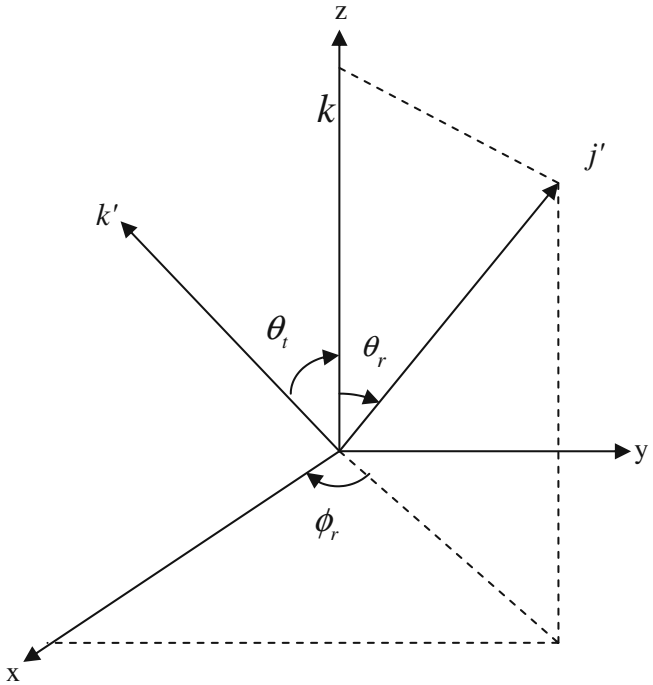

Figure 1. Schematic illustration of the center of mass frame used in this study.

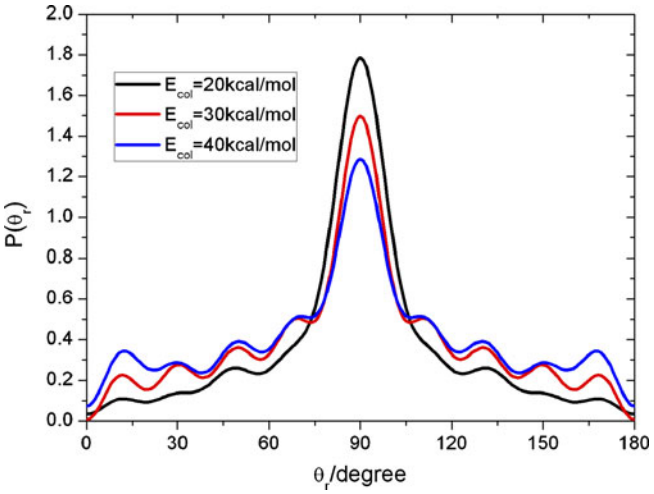

Figure 2. The $P(\theta_r)$ distributions at the three collision energies of 20, 30 and 40 kcal/mol for initial rotational and vibrational state of v = 0, j = 0 of the FCl molecule.

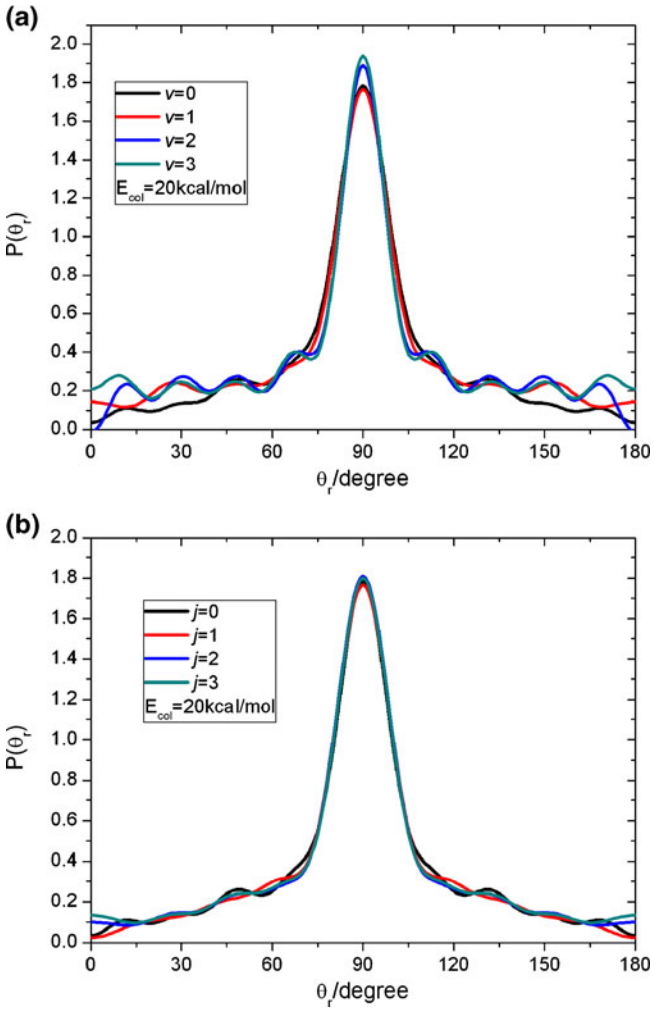

Figure 3. The $P(\theta_r)$ distribution at the collision energy of 20 kcal/mol and for initial rotational and vibrational states (**a**) v = 0–3, j = 0, (**b**) v = 0, j = 0–3.

product alignment along the y-axis and a marked product orientation pointing to the negative direction of the y-axis. These results mean that the product HCl molecules rotate clockwisely in the plane parallel to the scattering z–x plane. With an increase of the collision energy (figure 4), there are rather small but discernible changes in the calculated $P(\phi_r)$ distributions. This represents that the peak for ϕ_r=270° becomes somewhat lower when the collision energy changes from 20 kcal/mol to 30 kcal/mol or 40 kcal/mol. Therefore, influence of the collision energy on the product polarization $P(\phi_r)$ is rather insignificant. Comparisons of the $P(\phi_r)$ distributions for the different initial rotational and vibrational states at 20 kcal/mol collision energy (figures 5a and b) further reveal that the product polarization is insensitive to the initial vibrational and rotational excitations of the FCl.

The asymmetric feature of the $P(\phi_r)$ distributions observed here can be explained by the proposed impulse model for a triatomic system.[44] In the model, the relationship of the product angular momentum $\boldsymbol{j'}$ with the reagent orbital angular momentum $\boldsymbol{L}$ and reagent angular momentum $\boldsymbol{j}$ is described by a formula $j' = L\sin^2\beta + j\cos^2\beta + J_1 m_{Cl}/m_{HCl}$. $J_1 = \sqrt{\mu_{FCl}E_r}$ $(r_{HCl} \times r_{FCl})$, where E_r is the repulsive energy, r_{HCl} and r_{FCl} denote the unit vectors with Cl pointing to H and F, and μ_{FCl} is the reduced mass of the FCl molecule. The first two terms in the formula are symmetric, while the third term is asymmetric due to the effect of the repulsive energy and the reduced mass of FCl. As a consequence, the asymmetric feature is formed by the third term, which leads to the preference of clockwise rotation for the product HCl molecule in the title reaction.

The PDDCSs with kq=(0, 0) and (2, 0) are presented in figure 6 for the initial rotational and vibrational state of v=0, j=0 at the three collision energies of 20, 30, and 40 kcal/mol, respectively. For simplicity, we use $PDDCS_{00}$ and $PDDCS_{20}$ to denote the above two kinds of PDDCSs. It is observed (figure 6) that $PDDCS_{20}$ displays an opposite trend to that of $PDDCS_{00}$ within the whole range of the scattering angles for each of collision energy. This indicates a rather strong product alignment perpendicular to $\boldsymbol{k}$, and is consistent with the $P(\theta_r)$ distribution. The $PDDCS_{00}$, i.e., the usual differential cross section, shows that the product HCl molecules formed on the ground electronic state are mainly backward scattered, which is consistent with an abstraction mechanism under the title reaction. As indicated by the broader and lower distribution of the $PDDCS_{00}$ with increasing collision energy, such backward scattering is reduced with an increase of collision energy. For the scattering angles of 110°~130° and the collision energy of

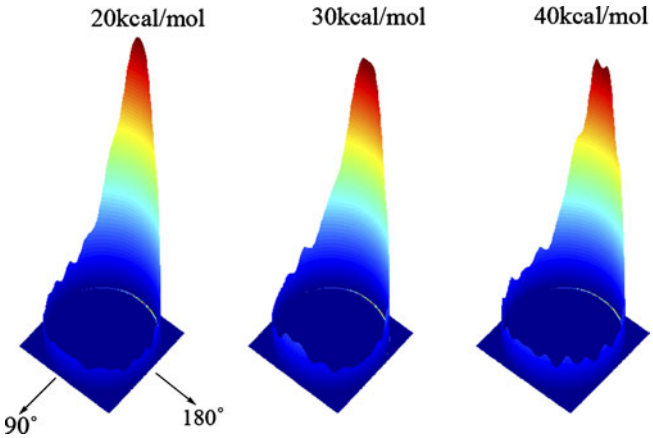

Figure 4. The $P(\phi_r)$ distributions at the three collision energies for initial rotational and vibrational state v=0 and j=0 for the FCl molecule.

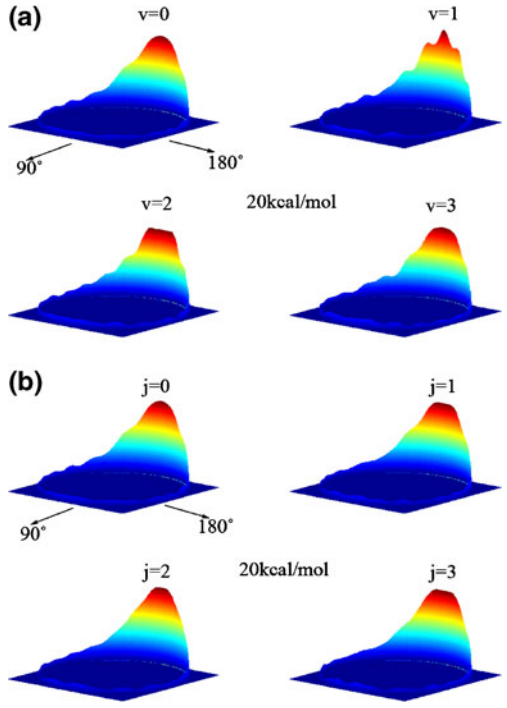

Figure 5. The $P(\phi_r)$ distribution at the collision energy of 20 kcal/mol and for initial rotational and vibrational states (**a**) $v = 0$–3, $j = 0$ (**b**) $v = 0$, $j = 0$–3.

20 kcal/mol, the $PDDCS_{20}$ approaches to its classical limited value of −0·5. More the value of the $PDDCS_{20}$ approaches to −0·5, the stronger the product aligns along the direction perpendicular to ***k***. Therefore, we can say that the product alignments are stronger for the scattering angles located within the above range. The values of the $PDDCS_{20}$ move far away from the

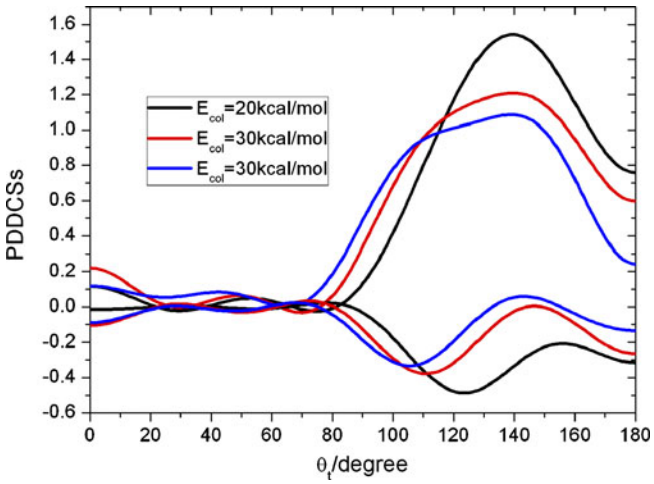

Figure 6. The polarization dependent differential cross sections ($PDDCS_{00}$ and $PDDCS_{20}$) at the three collision energies of 20, 30 and 40 kcal/mol.

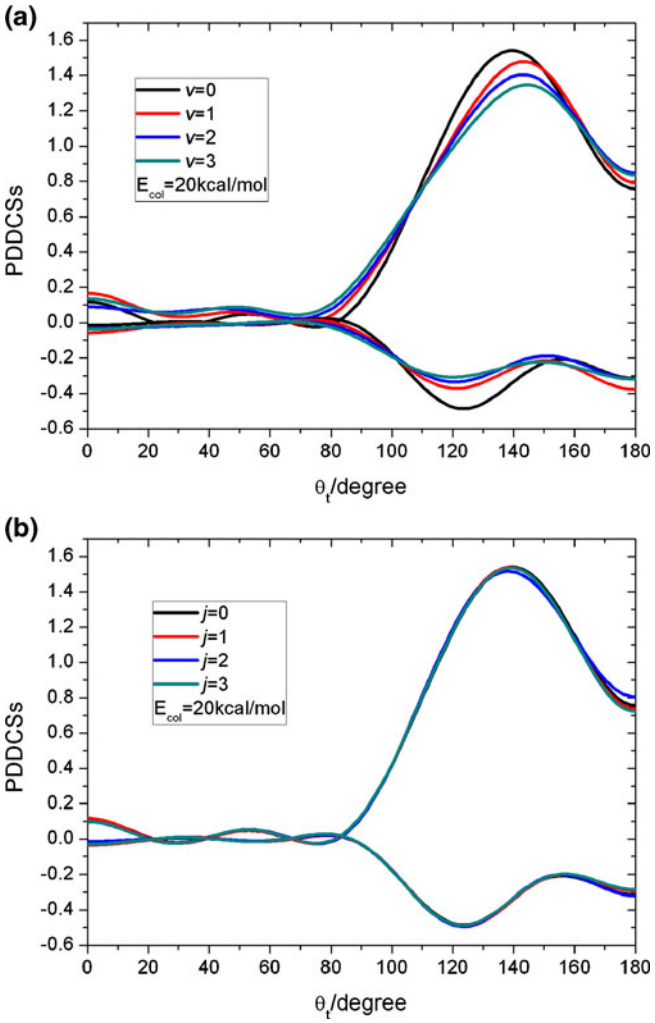

Figure 7. $PDDCS_{00}$ and $PDDCS_{20}$ at the collision energy of 20 kcal/mol and for initial rotational and vibrational states (**a**) $v = 0$–3, $j = 0$, (**b**) $v = 0$, $j = 0$–3.

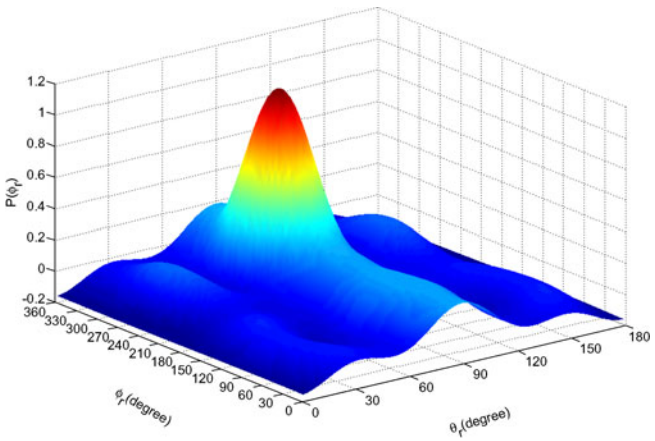

Figure 8. The $P(\theta_r,\phi_r)$ distribution at the collision energy of 20 kcal/mol and for initial rotational and vibrational state $v = 0$, $j = 0$ of the FCl molecule.

limited value of −0·5 as the collision energy increases. This suggests that the product alignments perpendicular to $\boldsymbol{k}$ become weaker with increasing energy. As illustrated in figure 6, the wave shape of the $PDDCS_{20}$ distribution also revealed the anisotropic feature of the product HCl. Figures 7a and b reveal the effect of the initial vibrational and rotational excitations of FCl on the $PDDCS_{00}$ and $PDDCS_{20}$ distributions. From figure 7a it can be seen that the initial vibration excitation of FCl reduces the product backward scattering and causes the $PDDCS_{20}$ to deviate from its limited value. As a result, the product alignments tend to be weaker at high vibration levels. Nevertheless, the initial rotational excitation has almost no influence on the $PDDCS_{00}$ and $PDDCS_{20}$ distributions (depicted in figure 7b).

The calculated $P(\theta_r,\phi_r)$ distributions are shown in figure 8 in the polar form for the collision energy of 20 kcal/mol and initial rotational and vibrational state of $v = 0$ and $j = 0$. Obviously, there is only one sharp peak at $(\theta_r, \phi_r) = (90°, 270°)$, which is in accordance with previous illustrations by the $P(\theta_r)$ and $P(\phi_r)$ distributions. The topographical feature of the $P(\theta_r,\phi_r)$ distributions further confirms and evidences the stereodynamics information of the title reaction. Other $P(\theta_r,\phi_r)$ distributions provide similar information and are not presented here. Further experimental and theoretical work is still necessary for better understanding its reaction mechanism.[45–51]

4. Conclusions

QCT calculations have been performed to investigate the chemical stereodynamics information of the title reaction. By running a batch of 50 000 trajectories on recently developed DHTSN ground PES of $1^2A'$ state, we presented the $P(\theta_r)$, $P(\phi_r)$, PDDCSs, and $P(\theta_r,\phi_r)$ distributions in the CM frame. The calculated results suggest that, for the initial rotational and vibrational state of $v = 0$ and $j = 0$ and the collision energies of 20, 30, and 40 kcal/mol, the HCl product exhibit a rather strong alignment perpendicular to the scattering z–x plane and a strong orientation pointing to the negative y-axis. The asymmetric behaviour of the $P(\phi_r)$ distribution was observed and explained by using the repulsive model proposed by Han *et al*. For the fixed collision energy of 20 kcal/mol, the effect of the initial rotational and vibrational excitations of the reagent FCl molecule on the polarization behaviours were investigated in detail. It was found that the initial rotational excitation is insensitivity to the polarization behaviour, but the initial vibrational excitations lead to a rather weaker product polarization and reduced the product backward scattering. For the invariably initial rotational and vibrational state of $v = 0$ and $j = 0$, the effect of different collision energies on the calculated quantities was also studied in detail. The results demonstrate that the $P(\theta_r)$ and $PDDCS_{20}$ distributions become weaker with increasing collision energy, while the $P(\phi_r)$ distribution is almost identical with an increase of the collision energy. As far as we know, the present work is the first chemical stereodynamics investigation on the H + FCl → HCl + F reaction.

Acknowledgements

The authors thank Professor Keli Han for providing us the benchmark stereodynamics code to do the present calculation. This work is supported by the National Natural Science Foundation of China (Grant 21003062) and Yong Funding of Jining University (No. 2009QNKJ02).

References

1. Sayós R, Hernando J, Hijazo J and Gonzalez M 1999 *Phys. Chem. Chem. Phys.* **1** 947
2. Kornweitz H and Persky A. 2004 *J. Phys. Chem. A* **108** 140
3. Fishchuk A V, Wormer P E S and Avoird A 2006 *J. Phys. Chem. A* **110** 5273
4. Deskevich M P, Hayes M Y, Takahashi K, Skodje R T and Nesbitt D J 2006 *J. Chem. Phys.* **124** 224303
5. Tang B Y, Yang B H, Han K L, Zhang R Q and Zhang J Z H, 2000 *J. Chem. Phys.* **113** 10105
6. Hayes M Y, Deskevich M P, Nesbitt D J, Takahashi K and Skodje R T 2006 *J. Phys. Chem. A* **110** 436
7. Sun Z G, Lee S Y and Zhang D-H 2007 *Chin. J. Chem. Phys*. **20** 365
8. Quéméner G and Balakrishnan N 2008 *J. Chem. Phys*. **128** 224304
9. Ding A M G, Kirsch L J, Perry D S, Polanyi J C and Schreiber J L 1973 *Faraday Discuss. Chem. Soc.* **55** 252
10. Beadle P, Dunn M R, Jonathan N B H, Liddy J P and Naylor J C 1978 *J. Chem. Soc., Faraday Trans.* **274** 2170
11. Würzberg E and Houston P L 1980 *J. Chem. Phys.* **72** 5915
12. Merritt J M, Küpper J and Miller R E 2005 *Phys. Chem. Chem. Phys.* **7** 67
13. Zolot A M and Nesbitt D J 2007 *J. Chem. Phys.* **127** 114319
14. L. P. Ju, Han K L and Zhang J Z H 2009 *J. Comput. Chem.* **30** 305

15. Aquilanti V, Cavalli S, Fazio D De, Simoni A and Tscherbul T V 2005 *J. Chem. Phys.* **123** 054314
16. Yang B H, Gao H T, Han K L and Zhang J Z H 2000 *J. Chem. Phys.* **113**, 1434
17. Xie T X, Zhang Y, Zhao M Y and Han K L 2003 *Phys. Chem. Chem. Phys.* **5** 2034
18. Chichinin A I, Gericke K H, Kauczok S and Maul C 2009 *Int. Rev. Phys. Chem.* **28** 607
19. Chu T S, Zhang Y and Han K L 2006 *Int. Rev. Phys. Chem.* **25** 201
20. Lique F, Alexander M H, Li G L, Werner H J, Nizkorodov S A, Harper W W and Nesbitt D J 2008 *J. Chem. Phys.* **128** 084313
21. Chu T S and Han K L 2008 *Phys. Chem. Chem. Phys.* **10** 2431
22. Sanov A and Mabbs R 2008 *Int. Rev. Phys. Chem.* **27** 53
23. Ghosala S and Mahapatra S 2004 *Chem. Phys. Lett.* **394** 207
24. Mahapatra S 2004 *Int. Rev. Phys. Chem.* **23** 483
25. Ghosal S and Mahapatra S 2005 *J. Phys. Chem. A* **109** 1530
26. Ghosal S and Mahapatra S 2004 *J. Chem. Phys.* **121** 5740
27. Ghosal S and Mahapatra S 2007 *J. Photochem. Photobiol. A* **190** 161
28. Mahapatra S 2009 *Acc. Chem. Res.* **42** 1004
29. Han K L, He G Z and Lou N Q 1996 *J. Chem. Phys.* **105** 8699
30. Han K L, Zhang L, Xu D L, He G Z and Lou N Q 2001 *J. Phys. Chem. A* **105** 2956
31. Wang M L, Han K L and He G Z 1998 *J. Phys. Chem. A* **102** 10204
32. Chen M D, Han K L and Lou N Q 2003 *J. Chem. Phys.* **118 4463**
33. Han K L and He G Z 2007 *J. Photochem. Photobiol. C Photochem. Rev.* **8** 55
34. Han K L, He G Z and Lou N Q 1993 *Chin. Chem. Lett.* **4** 517
35. Aquilanti V, Bartolomei M, Pirani F, Cappelletti D, Vecchiocattivi F, Shimizu Y and Kasai T 2005 *Phys. Chem. Chem. Phys.* **7** 291
36. Aquilanti V, Pirani F, Cappelletti D, Vecchiocattivi F and Kasai T 2004 *Theory of chemical reaction dynamics* **145** 243 (Springer, Netherland)
37. Aoiz F J, Herrero V J, Miranda M P de and Rabanos V S 2007 *Phys. Chem. Chem. Phys.* **9** 5367
38. Aoiz F J, Herrero V J, Rabanos V S and Verdasco J E 2004 *Phys. Chem. Chem. Phys.* **6** 4407
39. Gonzalez-Sanchez L, Gomez-Carrasco S, Aguado A, Paniagua M, Hernandez M L, Alvarino J M and Roncero O 2004 *Mol. Phys*. **102** 2381
40. Gomez-Carrasco S, Roncero O, Gonzalez-Sanchez L, Hernandez M L, Alvarino J M, Paniagua M and Aguado A 2005 *J. Chem. Phys.* **123** 114310
41. Balint-Kurti G G and Vasyutinskii O S 2009 *J. Phys. Chem. A* **113** *14281*
42. Piermarini V, Lagana A and Balint-Kurti G G 2001 *Phys. Chem. Chem. Phys.* **3** 4515
43. Balint-Kurti G G 2008 *Int. Rev. Phys. Chem.* **27** 507
44. Li R J, Han K L, Li F E, Lu R C, He G Z and Lou N Q 1994 *Chem. Phys. Lett.* **220** 281
45. Szalewicz K 2008 *Int.Rev. Phys. Chem.* **27** 273
46. Reisler H and Krylov A I 2009 *Int. Rev. Phys. Chem.* **28** 267
47. Lourderaj U, Park K and Hase W L 2008 *Int. Rev. Phys. Chem.* **27** 361
48. Gou F, Kleyn A W and Gleeson M A 2008 *Int. Rev. Phys. Chem.* **27** 273
49. Braams B J and Bowman J M 2009 *Int. Rev. Phys. Chem.* **28** 577
50. Bernath P F 2009 *Int. Rev. Phys. Chem.* **28** 681
51. Gerber R B and Sebek J 2009 *Int. Rev. Phys. Chem.* **28** 207